International Journal of GEOMATE, Jan., 2021, Vol.20, Issue 77, pp. 163-172
ISSN: 2186-2982 (P), 2186-2990 (O), Japan, DOI: https://doi.org/10.21660/2021.77.98264
Geotechnique, Construction Materials and Environment

LOCAL SCOUR AROUND T-SHAPE SUBMERGED GROYNES IN CLEARWATER CONDITIONS

Budoor Mohammed Rashak and Saleh Issa Khassaf
College of Engineering, University of Basrah, Iraq

*Corresponding Author, Rreceived: 18 Aug. 2020, Revised: 08 Sep. 2020, Accepted: 05 Dec. 2020

ABSTRACT: A series of failures due to bank erosion have rekindled our understanding of the scour phenomena. One of the methods to improve the bank's protection against scour are river training structures, such as submerged groynes, where installed in a river to relieve erosion in the outer bank in two consecutive bends. Under clear water conditions, the maximum scour depth based on laboratory experiments around T-shape submerged groynes was investigated, and the most parameters that reduce the scour around these obstructions were also investigated. The result of T-shape submerged groynes showed that decreasing of scour depth ratio due to the increasing submerged ratio, and the number of groynes. The scour hole geometry will increase with the Froude number, flow intensity, and the spacing between groynes. A new empirical equation was derived and showed a correlation between the predicted results with the observed experiments.

Keywords: Submerged Groyne, River training structures, Clearwater Conditions, Bed Topography Pattern

1. INTRODUCTION

Scour has been known as a severe risk to the performance of flowing water in any river. The scour phenomenon can be defined as a natural reduction quantity under supposed designated level (generally the river bed level before incipience of scouring). Furthermore; it can occur under each flow state but the scour impact is higher in the condition of a larger flow. The advantages of scouring and fill in the riverbed during a flood have an important relation to the river bank stability [1]. Goynes are the hydraulic structures that have functions of protecting bank erosion and maintaining water level through deflecting flow direction, a series of groynes in a row may also be placed on one side or both sides of a river to form a groyne field, commonly utilized in river engineering to avoid bank erosion and control river meandering [2].

The total scours for any stream can be categorized into three major types: general scour and localized scour, where the latest has also divided into sub-divisions of scour, namely contraction and local scour [3]. The general scour defined as the exclusion of sediments from the river bed by the flowing stream and lowering the river bed that observe as a response for increasing flow discharge [4]. It can further be divided into long-term and short-term scour that are differentiated by the period development of the scour hole, short – term general scour occurs due to single or several closely spaced floods especially the size and time of concentration [5]. While localized scour: This type; counter to general scour is taken place due to the presence of hydraulic structures. On the other hand, it is divided into contraction scour and local scour [6]. The contraction scour is a lowering of the streambed across the stream or waterway bed at the groyne. Contraction scours results from constriction of the flow which results in the removal of material from the bed across all or most of the channel width [7].

The local scour is one of the most important concerns in the design and implementation of groynes. Local scour may occur for two distinct sediment transport conditions, clear water scour refers to local scour that occurs when the velocity of flow is less than the value needed to initiate sediment motion or critical velocity on the bed material upstream of the structure ($v \leq v_c$, where v_c is the critical mean velocity). Hence, the sediments are at rest. live bed scour refers to local scour that occurs when the velocity of flow exceeds the value necessary to initiate sediment motion (suspended and or bed load) upstream ($v > v_c$), however; the sediments are being transported by the flow [8] And obtained the critical shear velocity for 0.1 mm< d_{50} <1 mm as follows:

$$\boldsymbol{v_{*c} = 0.0115 + 0.0125(d_{50})^{1.4}} \quad \text{(a)}$$

On the other hand, proposed an equation for critical velocity by utilizing water depth (y)

$$\boldsymbol{v_c / v_{*_c} = 5.75\, log\ (5.53\, \frac{y}{d_{50}})} \quad \text{(b)}$$

The ratio of (v_*/v_{*c}) or (v/v_c) is defined as the (flow intensity) and give the beginning of sediment transfer. In result, we have methods to calculate critical velocity by using Eq.(a) to get the critical shear velocity and then substituting (v_{*c}) into Eq.(b)

to get the critical velocity, The flow velocity should be smaller than the critical flow velocity, and larger than half of the critical flow velocity, to achieve the clear flow condition [9].

2. THE EXPERIMENTAL FLUME

The flume used in this research, as illustrated in Fig.1. It is made of fibreglass reinforced plastic with steel reinforcement, with (5.64 m) long, (0.6 m) wide and has a height of (0.4 m). The flume included three sections:

The first section consists of an inlet tank located in the upstream of the flume with measurements of (0.2*1.17*0.6 m) for long, height and wide respectively, the second section of the flume is the working section consists of the rectangular weir (0.6 m) wide and (0.35 m) depth utilized to measure the flow discharge

Gravel and screens to distributed the flow uniformly over the width of the flume and. While In the middle, the layer of sand of (0.1 m) thickness, at the end of working section a sediment basin (0.4 m*0.3 m) for long and height respectively, the depth of flow is controlled by a tailgate provider with wheels level**.** The third section of the flume is a reservoir (0.75 m*1.17 m*0.6 m) for the long, height and wide respectively, which supply the water through a recirculating flume of the closed water system through a centrifugal pump.

The centrifugal pump attached with an electric motor of maximum capacity equals (8.4 l/sec). Flow depth was measure by using Point gauge with (± 0.1 mm) accuracy mounted on a carriage which can be moved transversely and longitudinally over the working section by a couple of parallel rails supported on the flume wall.

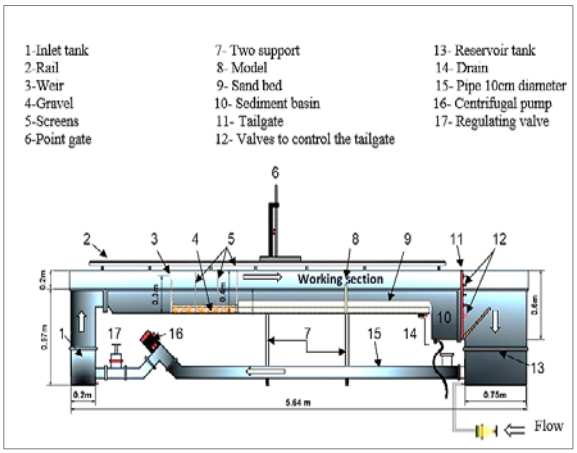

Fig.1 Detail drawing of a laboratory flume

3. THE EXPERIMENTAL MODELS

Submerged groyne T-shape type models were utilized in all the experiments, the models were made of polystyrene foam material of thickness (1) cm and height (H_g) (15) cm of which (5) cm is the net height (height of submerged groyne should have between 1/3 and 1/2 of flow depth) [10]. While; (20) cm projection length (L_g) (approximately not less than one-third of the flume width [11], and (10) cm is the projection length of the groyne which parallel to the flow direction (I) as appeared in Fig. 2.

.

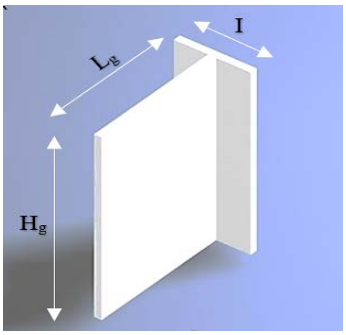

Fig.2 Sketches for the (T- shape) groynes models

4. THE BED MATERIALS

Mechanical sieve analysis was carried out to classify the sand bed material. The tests showed that the bed material consists of cohesionless sand with the mean partial size of (d_{50}= 0.3) mm, d_{50}, is taken as a median particle sediment size and the level of uniformity distribution particle size in this study is characterized by the geometric standard deviation of (σ_g = 1.32). σ_g is expressed as $\sigma_g=\sqrt{(d_{84}/d_{16})}$, it is usually accepted that the sediment may be considered uniform if (σ_g <1.4) and no uniform else [12]. Fig. 3 explains the grain size distribution curve.

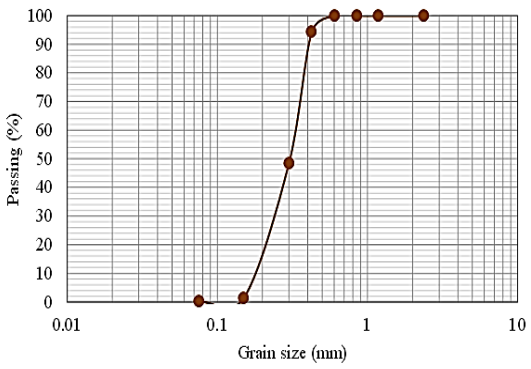

Fig.3 Distribution curve of grain size for bed material (d_{50}=0.3mm)

5. ANALYSIS AND DISCUSSION OF

Discussing and analyzing the results acquired from the laboratory data is a more important step in designing the submerged groynes, to decrease the effect of scour depth phenomena. All the experimental work was performed in steady subcritical flow and clear water conditions. All the experimental results utilized in the study are listed in Table 1.

Table 1 The experimental results

Run No.	h_0 (cm)	h_1 (cm)	v (m/s)	v_c (m/s)	b (cm)	n	Fr	v/v_c	h_1/h_0	b/h_0	ds (cm)	ds/h_0
Tested intensity of flow and submerged ratio using single T-shape groyne												
1	7.5	2.5	0.179	0.250	0	1	0.208	0.716	0.33	0.0	7.1	0.95
2	7.5	2.5	0.165	0.250	0	1	0.192	0.660	0.33	0.0	5.9	0.79
3	7.5	2.5	0.154	0.250	0	1	0.180	0.619	0.33	0.0	5.1	0.68
4	7.5	2.5	0.144	0.250	0	1	0.168	0.578	0.33	0.0	4.2	0.56
5	7.5	2.5	0.131	0.250	0	1	0.153	0.526	0.33	0.0	3.8	0.51
6	11	6	0.179	0.263	0	1	0.172	0.680	0.55	0.0	3.9	0.35
7	10	5	0.179	0.259	0	1	0.180	0.689	0.50	0.0	5	0.50
8	9	4	0.179	0.256	0	1	0.190	0.699	0.44	0.0	5.7	0.63
9	8	3	0.179	0.252	0	1	0.202	0.710	0.38	0.0	6.5	0.81
10	7	2	0.179	0.247	0	1	0.216	0.723	0.29	0.0	7.4	1.06
Tested the different spacing between two T-shape groynes for three times (Lg, 1.5Lg, 2Lg)												
11	7.5	2.5	0.179	0.250	40	2	0.208	0.716	0.33	5.3	6	0.80
12	7.5	2.5	0.165	0.250	40	2	0.192	0.660	0.33	5.3	4.8	0.64
13	7.5	2.5	0.154	0.250	40	2	0.180	0.619	0.33	5.3	4.2	0.56
14	7.5	2.5	0.144	0.250	40	2	0.168	0.578	0.33	5.3	3.5	0.47
15	7.5	2.5	0.131	0.250	40	2	0.153	0.526	0.33	5.3	2.8	0.37
16	11	6	0.179	0.263	40	2	0.172	0.680	0.55	3.6	2.9	0.26
17	10	5	0.179	0.259	40	2	0.180	0.689	0.50	4.0	4	0.40
18	9	4	0.179	0.256	40	2	0.190	0.699	0.44	4.4	4.8	0.53
19	8	3	0.179	0.252	40	2	0.202	0.710	0.38	5.0	5.8	0.73
20	7	2	0.179	0.247	40	2	0.216	0.723	0.29	5.7	6.3	0.90
21	7.5	2.5	0.179	0.250	30	2	0.208	0.716	0.33	4.0	5.5	0.73
22	7.5	2.5	0.165	0.250	30	2	0.192	0.660	0.33	4.0	4.6	0.61
23	7.5	2.5	0.154	0.250	30	2	0.180	0.619	0.33	4.0	4.2	0.56
24	7.5	2.5	0.144	0.250	30	2	0.168	0.578	0.33	4.0	3.2	0.43
25	7.5	2.5	0.131	0.250	30	2	0.153	0.526	0.33	4.0	2.5	0.33
26	11	6	0.179	0.263	30	2	0.172	0.680	0.55	2.7	2.5	0.23
27	10	5	0.179	0.259	30	2	0.180	0.689	0.50	3.0	3.6	0.36
28	9	4	0.179	0.256	30	2	0.190	0.699	0.44	3.3	4.3	0.48
29	8	3	0.179	0.252	30	2	0.202	0.710	0.38	3.8	5.2	0.65
30	7	2	0.179	0.247	30	2	0.216	0.723	0.29	4.3	5.9	0.84
31	7.5	2.5	0.179	0.250	20	2	0.208	0.716	0.33	2.7	5	0.67
32	7.5	2.5	0.165	0.250	20	2	0.192	0.660	0.33	2.7	4	0.53
33	7.5	2.5	0.154	0.250	20	2	0.180	0.619	0.33	2.7	3.6	0.48
34	7.5	2.5	0.144	0.250	20	2	0.168	0.578	0.33	2.7	2.5	0.33
35	7.5	2.5	0.131	0.250	20	2	0.153	0.526	0.33	2.7	2	0.27
36	11	6	0.179	0.263	20	2	0.172	0.680	0.55	1.8	2.1	0.19
37	10	5	0.179	0.259	20	2	0.180	0.689	0.50	2.0	3.1	0.31
38	9	4	0.179	0.256	20	2	0.190	0.699	0.44	2.2	3.8	0.42

Table 1 Continued

39	8	3	0.179	0.252	20	2	0.202	0.710	0.38	2.5	4.6	0.58
40	7	2	0.179	0.247	20	2	0.216	0.723	0.29	2.9	5.6	0.80
	Tested the different spacing between three T-shape groynes for three times (Lg, 1.5Lg, 2Lg)											
41	7.5	2.5	0.179	0.250	40	3	0.208	0.716	0.33	5.3	5.7	0.76
42	7.5	2.5	0.165	0.250	40	3	0.192	0.660	0.33	5.3	4.5	0.60
43	7.5	2.5	0.154	0.250	40	3	0.180	0.619	0.33	5.3	4	0.53
44	7.5	2.5	0.144	0.250	40	3	0.168	0.578	0.33	5.3	3.3	0.44
45	7.5	2.5	0.131	0.250	40	3	0.153	0.526	0.33	5.3	2.5	0.33
46	11	6	0.179	0.263	40	3	0.172	0.680	0.55	3.6	2.7	0.25
47	10	5	0.179	0.259	40	3	0.180	0.689	0.50	4.0	3.8	0.38
48	9	4	0.179	0.256	40	3	0.190	0.699	0.44	4.4	4.4	0.49
49	8	3	0.179	0.252	40	3	0.202	0.710	0.38	5.0	5.5	0.69
50	7	2	0.179	0.247	40	3	0.216	0.723	0.29	5.7	6	0.86
51	7.5	2.5	0.179	0.250	30	3	0.208	0.716	0.33	4.0	5.2	0.69
52	7.5	2.5	0.165	0.250	30	3	0.192	0.660	0.33	4.0	4.3	0.57
53	7.5	2.5	0.154	0.250	30	3	0.180	0.619	0.33	4.0	3.8	0.51
54	7.5	2.5	0.144	0.250	30	3	0.168	0.578	0.33	4.0	3	0.40
55	7.5	2.5	0.131	0.250	30	3	0.153	0.526	0.33	4.0	2.2	0.29
56	11	6	0.179	0.263	30	3	0.172	0.680	0.55	2.7	2.3	0.21
57	10	5	0.179	0.259	30	3	0.180	0.689	0.50	3.0	3.4	0.34
58	9	4	0.179	0.256	30	3	0.190	0.699	0.44	3.3	4.1	0.46
59	8	3	0.179	0.252	30	3	0.202	0.710	0.38	3.8	5	0.63
60	7	2	0.179	0.247	30	3	0.216	0.723	0.29	4.3	5.4	0.77
61	7.5	2.5	0.179	0.250	20	3	0.208	0.716	0.33	2.7	4.5	0.60
62	7.5	2.5	0.165	0.250	20	3	0.192	0.660	0.33	2.7	3.6	0.48
63	7.5	2.5	0.154	0.250	20	3	0.180	0.619	0.33	2.7	3.3	0.44
64	7.5	2.5	0.144	0.250	20	3	0.168	0.578	0.33	2.7	2.1	0.28
65	7.5	2.5	0.131	0.250	20	3	0.153	0.526	0.33	2.7	1.7	0.23
66	11	6	0.179	0.263	20	3	0.172	0.680	0.55	1.8	2	0.18
67	10	5	0.179	0.259	20	3	0.180	0.689	0.50	2.0	2.9	0.29
68	9	4	0.179	0.256	20	3	0.190	0.699	0.44	2.2	3.5	0.39
69	8	3	0.179	0.252	20	3	0.202	0.710	0.38	2.5	4.3	0.54
70	7	2	0.179	0.247	20	3	0.216	0.723	0.29	2.9	5.1	0.73

5.1 Effect of Flow Intensity (v/v_c) on the Local Scour (ds/h_0)

The intensity of flow considers significant parameter that effect on the scours process around submerged groynes. To clarify this case, sets of experiments were carried out to establish the relationship between the scour depth ratio (ds/h_0), and the intensity of flow (v/v_c) for the different number of the submerged groyne and (b=40 cm). The obtained results are shown in Fig. 4 It can be observed from the figure above; that depth of scouring ratio increased linearly with flow intensity increasing for velocities below the threshold value.

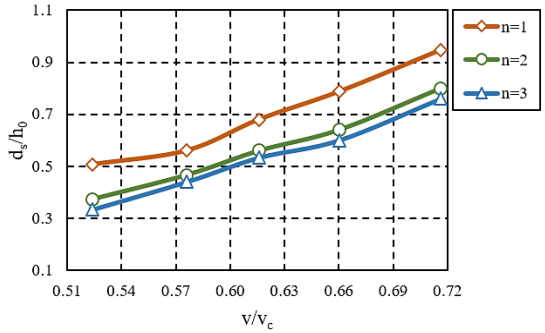

Fig.4 Effect of flow intensity (v/v_c) on scour depth ratio (ds/h_0) with the different number of submerged groynes for spacing (b = 40 cm)

Some experiments are selected on the form of photos to show the scour process around submerged groynes, as presented in Fig. 5.

It can be observed that the flow intensity will increase the scour depth width and volume and the location of the hole, this may be attributed to the increase in separation region that located in the downstream side of the submerged groyne so more vortices will be formed that in turn cause more scour.

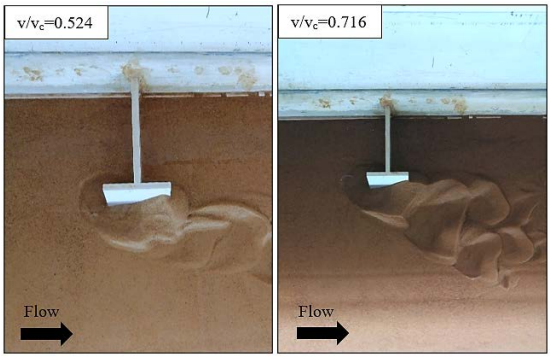

Fig.5 Photos that clarify the effect of intensity of flow (v/v_c) on the ratio of scour depth development (ds/h_0) for single T-shape groyne

5.2 Effect of Submerged Ratio (h_1/h_0) on the Local Scour (ds/h_0)

To study the influence of submerged ratio (h_1/h_0) on the maximum scour depth ratios (ds/h_0) for the different number of the submerged groyne and (b=40 cm). A set of experiments were curried for the purpose to reduce the effect of scouring phenomena, all the experiment results are illustrated in Fig. 6.

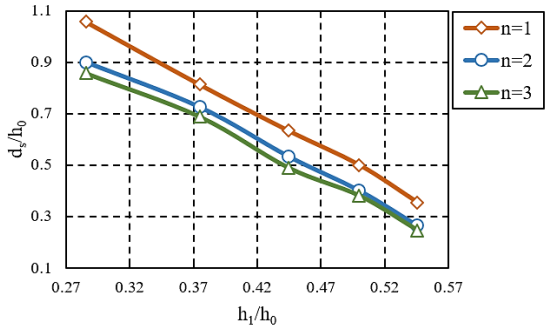

Fig.6 Effect of submerged ratio (h_1/h_0) on scour depth ratio (ds/h_0) with the different number of submerged groynes for spacing (b = 40 cm)

From the Fig.6, it is shown that the overtopping flow does make a significant difference in the value of a scour hole, in which increasing the submerged ratio, is inversely proportional to the scour hole ratio.

It is observed that, under the same flow condition, the depth of scouring reduces due to increasing the flow depth, and also, It is evident that due to the re-circulatory motions practically absent near the free surface at high submergence levels, and it will decrease the ability of horseshoe vortices to pick up and entrain sediments. So; when there flows that can be described as deep; the holes of local scour are decreased until they become having invisible efficiency, while it presents in low submergence level case strongly near the free surface causing an increase of scour hole.

5.3 Effect of Froude Number (Fr) on the Local Scour (ds/h_0)

Froude number considers the most important parameters effected on the scour process around the submerged groyne. Different experiments were conducted to reduce the impact of Froude number (Fr) on the ratio of scour depth (ds/h_0) for a different number of the submerged groyne and (b=40 cm), and the obtained results for these experiments has been shown in Fig.7.

It has been noticed from the figure that the scour depth increases with increasing Froude number based on the law of Froude number that is evident from it that the scour depth increase with increasing the velocity of flow and decreasing in scour depth will increase Froude number value leading to increase the scour depth geometry at a constant flow depth.

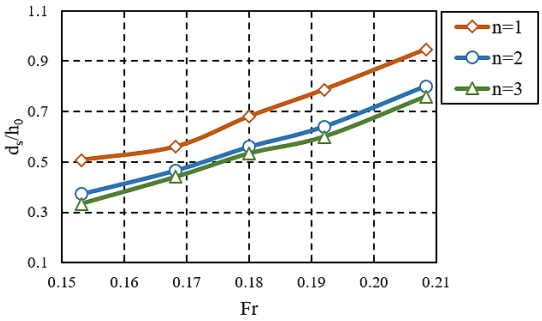

Fig.7 Effect of Froude number (Fr) on scour depth ratio (d_s/h_0) for the different number of submerged groynes for spacing (b = 40 cm)

Fig.8 presents the effect of increasing Froude number from (0.121 to 0.208), It can be seen that scour phenomena carry out in a wider and larger area, also; when (Fr=0.34) the fewer sediments were distributed around the scour hole with small

camber, while, when (Fr=0.49); the sediments will collect around the scour depth sides with very high camber, then the sediments starts to decrease and gradually disappear at the far downstream of the groyne.

Fig.8 Photos that clarify the effect of Froude number (Fr) on the ratio of scour depth development (ds/h_0) for single T-shape groyne

5.4 Effect of A Number of the Groyne (n) on the Local Scour (ds/h_0)

Scientific experiments have been conducted to determine the relationship between the scour depth ratio (ds/h_0) and a number of the submerged groyne (n) for different Froude number, all results of these experiments are shown in Fig. 9. It was observed from the figure; the depth of scour was reduced highly for the first groyne at the nose of the upstream side. And also observed that the scour region has deeper with much wider space for one groyne than that of two groynes and three groynes.

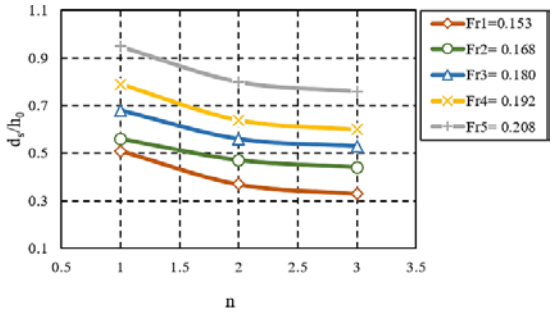

Fig.9 influence the number of the groynes (n) on scour depth ratio (ds/h_0) for different Froude number

This result is illustrated clearly in Fig.10. The scour in upstream of its nose which higher level of deposition in downstream, while the deposition area starts in a long-distance toward the downstream for one groyne, The decreasing percentage in scour depth when an increasing number of groynes from one to two was range about (15.5) %, (22.5) %, and (29.6) % for spacing between groynes ($2L_g$, $1.5L_g$, and L_g) respectively. While it was range about (5) %, (5.5) % and (10) % when increasing groynes number from two to three with the same three spacing between groynes. The successive vortices overlapping which resulted from the successive groynes where this causes for reducing the strength of the horseshoe vortex which is proportional to groynes number.

Fig.10 Photos that clarify the effect of groynes configuration (n) on the ratio of scour depth development (ds/h_0)

5.5 Effect of Spacing Between Groynes (b/h_0) on the Local Scour (ds/h_0)

The scouring process has been directly influenced by the spacing between submerged groynes. Six of the experiments were done for evaluating the relationship between spacing and the scour geometry. The results have been plotted to relate the spacing between the groynes (b/h_0) with scouring depth ratio (ds/h_0) which is a dimensionless fraction as shown in Fig.11.

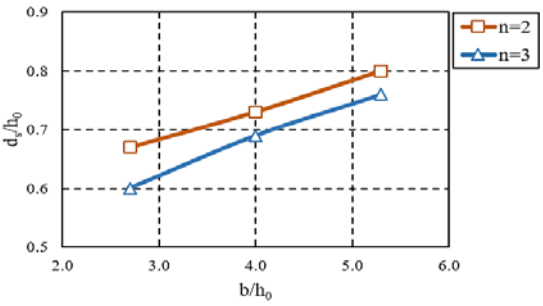

Fig.11 Impact of spacings between groynes (b/h_0) on development of scour depth ratio (ds/h_0) for (T-Shape) type

It can be shown from the figure above that the scouring depth development is higher when increasing the groynes spacing and lower when reducing the spacing between them, due to the interference between horseshoe vortex. The

decreasing percentage in the scour hole was measured to be about (8.3) % and (8.8) % for decreasing the spacing between groynes from ($2L_g$) to ($1.5L_g$). Besides, it was range about (9.1) % and (13.5) % when reducing the spacing from ($1.5L_g$) to (L_g) under the same value of maximum Froude number.

6. BED TOPOGRAPHY PATTERN

After the end for chosen experiments of maximum Froud number (which most important parameter that effects on local scour), The results of the experiments with maximum Froude number are compared with scouring patterns for T-shaped submerged groynes. The data for bed sand topography levels were contoured using the computer software (Surfer 17). Fig. 12 to 15 illustrate the topography of scour holes and downstream sand bars. Each experiment has similar flow conditions, submerged groyne geometry, and soil properties; (v/v_c= 0.716, Fr= 0.208, and h_1/h_0=0.33). It was shown from these figures that the maximum scour depth ratio occurred at the nose of the submerged groyne. The height of the sand ripples behind the groyne was observed to be about (2.5–3.5) cm, also scour hole width and volume for single (T-shape) submerged groyne is larger than for those of second and third T-shape submerged groyne; respectively, while all models formed sand bars in the downstream, and also it was observed from the figures that when the spacing is the same as the length of the submerged groyne ($b=L_g$=20 cm); the sediments deposition starts to concentrate between the groynes and seems nearer to the following groyne. while when the spacing between the groynes increased to twice length of the groyne ($b=2L_g$) indicating the distance between them has little effect on the scour.

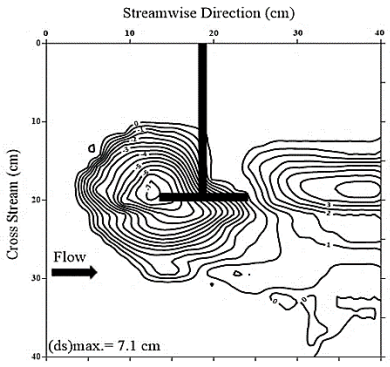

Fig.12 Contour Maps for Scouring Hole Geometry for Single T-Shape of the Submerged Groyne

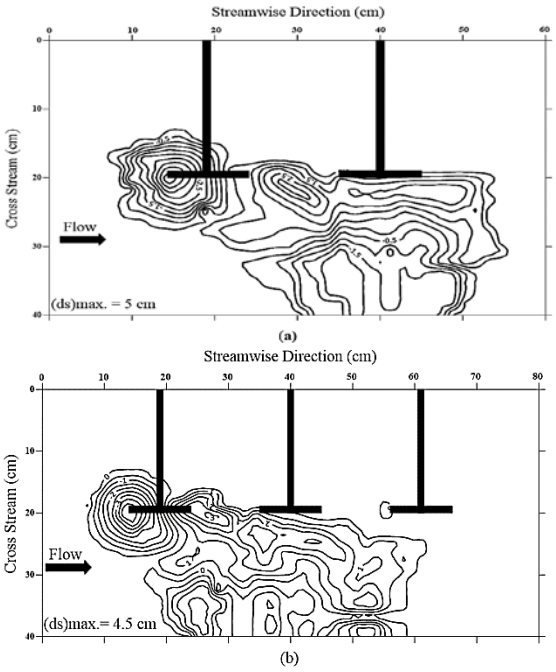

Fig.13 Contour maps of scour holes submerged groyne for the cases
(a) Two T-shape groyne with spacing between them b=20 cm
(b) Three T-shape groyne with spacing between them b=20 cm

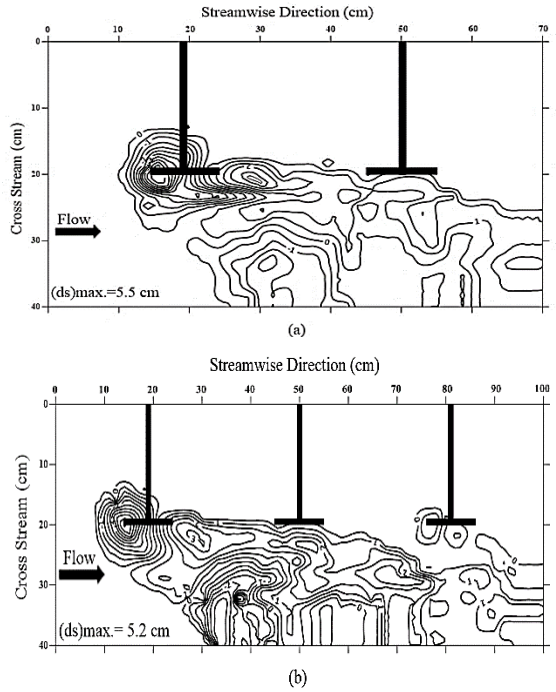

Fig.14 Contour maps of scour holes submerged groyne for the cases
(a) Two T-shape groyne with spacing between them b=30 cm
(b) Three T-shape groyne with spacing between them b=30 cm

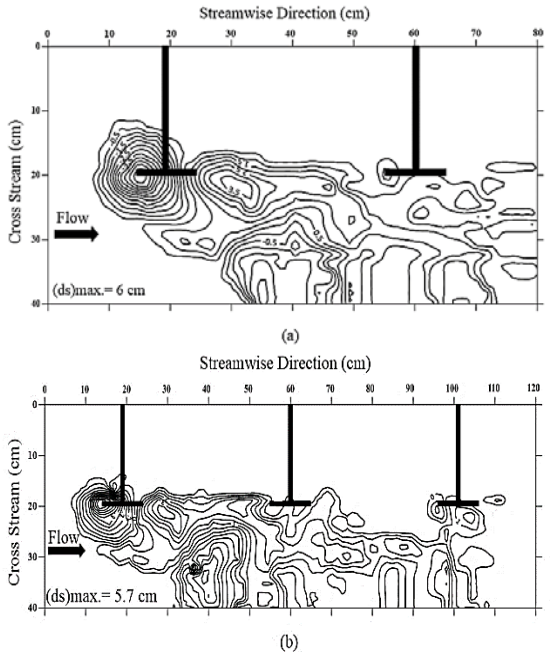

Fig.15 Contour maps of scour holes submerged groyne for the cases
(a) Two T-shape groyne with spacing between them b=40 cm
(b) Three T-shape groyne with spacing between them b=40 cm

7. DEVELOPMENT OF NEW FORMULA

Dimensional analysis is a mathematical technique used in study works for design and performing models' experiments. By using this method; the maximum scours depth ratio (ds_{max}) at T-shape submerged groyne under clear water conditions, the factional relationship may be written as:

$$d_{Smax=}f\{h_0, h_1, H_g, v, v_c, L_g, \rho, \rho_s, g, n, b, d_{50}, \mu, \sigma_g, B, S_\circ, I, \theta\} \quad (1)$$

The factors definitions are listed in Table (2). By applying the Buckingham's p theorem; After the simplification of the above relationship by dispensing with the terms with constant values and arrangements; Eq. (1) can be written as:

$$\frac{d_{Smax}}{h0} = f_5\left(\frac{v}{v_c}, \frac{h_1}{h_0}, Fr, n, \frac{b}{h_0}\right) \quad (2)$$

To develop Eq. (2) used to calculate the relative scour depth ratio (ds/h_0) based on the parameters of the non-dimensional formula, which describes an expression for maximum scour depth at the submerged groyne.

The (IBM SPSS Statistics 25) was used to make analysis the formula for T-shape of submerged groynes through non-linear regression analysis. The obtained expression involves different flow, and geometrical properties, which have an important effect on the local scour criteria. the developed equation is:

$$ds/h_0 = c_0 \times e^{(c_1 \times Fr)} + c_1 \times e^{\left(c_2 \times \frac{v}{v_c}\right)} + c_2 \times e^{\left(c_3 \times \frac{h_1}{h_0}\right)} + c_3 \times e^{\left(c_4 \times \frac{b}{h_0}\right)} + c_4 \times e^{(c_5 \times n)} \quad (3)$$

Where:

c_1=1.489	c_2=4.117	c_3=-3.292
c_4=0.002	c_5=0.747	c_6=-1.092

So, the equation becomes

$$ds/h_0 = 1.489 \times e^{(4.117 \times Fr)} + 4.117 \times e^{\left(-3.292 \times \frac{v}{v_c}\right)} - 3.292 \times e^{\left(0.002 \times \frac{h_1}{h_0}\right)} + 0.002 \times e^{\left(0.747 \times \frac{b}{h_0}\right)} + 0.747 \times e^{(-1.092 \times n)} \quad (4)$$

To this equation; the coefficient of determination (R^2) is (0.962). The above equations were derived utilizing (80) % of the experimental results, then the accuracy of these equations was tested by using other data (around (20) % of the residual data), these data are substituted in the Eq. (4) and their results were compared with the experimental results to show the predicted convergence to observed records between the predicted (ds/h_0) from the formulas) to the observed (ds/h_0) (from the experiments).

The value of the coefficient of determination (R^2=0.9777) is reflected good agreement for all data as shown in Fig.16.

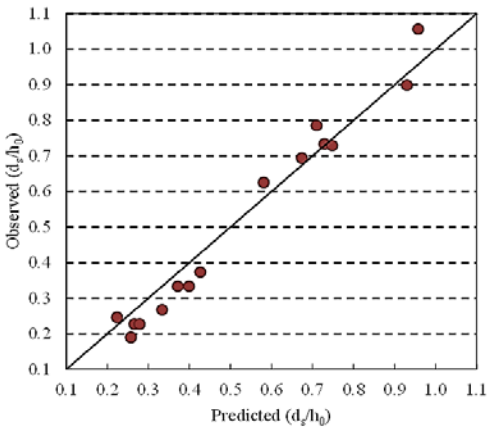

Fig.16 Validation of Eq. (4) for T-Shape submerged groyne with experimental data

Table 2 The parameters definitions using in dimensional analysis

symbol	Definition	Dimension
B	Flume width	L
I	Projection length of groyne parallel to the flow direction	L
L_g	Projection length of groyne	L
H_g	Height of groyne	L
d_{16}	Sediment size for which 16% of the particle are finer	L
d_{50}	Median particle grain size	L
d_{84}	Sediment size for which 84% of the particle are finer	L
d_S	local scour depth around the groynes	L
Fr	Froude number	-
g	Gravitational acceleration	LT^{-2}
n	Number of groynes	-
b	Spacing between the groynes	L
S_0	The slope of the channel bed	-
h_0	Flow water depth	L
h_1	Distance from the water surface to the top of the groyne	L
θ	The angle of groyne inclination	-
v	Mean velocity	LT^{-1}
v_c	Critical velocity	LT^{-1}
σ_g	Geometric standard deviation	-
μ	Dynamic viscosity of the fluid	$MT^{-1}L^{-1}$
ρ	Density of fluid	MT^{-3}
ρ_s	The density of the sediment	MT^{-3}

8. CONCLUSIONS

This study is focused on characterizing the diversity in the behaviour of the flow and bed topography near submerged groynes. The maximum scours depth geometry was observed to be at the upstream nose for T-shaped submerged groynesdue to the. The development of scour depth decreases due to increasing the submerged ratio, and a number of the groynes. while it increases the scour hole geometry with increasing of flow intensity, and Froude number, and spacing between the groyne. For similar experimental flow conditions of maximum Froude number.The decreasing percentage in scour depth when increasing number of groynes from one to two was range about (15.5) %, (22.5) %, and (29.6) % for spacing between groynes ($2L_g$, $1.5L_g$, and L_g) respectively. While it was range about (5) %, (5.5) %, and (10) % when increasing groynes number from two to three with the same three spacing between groynes. While the decreasing percentage in the scour hole was measured to be about (8.3) % and (8.8) % for decreasing the spacing between groynes from ($2L_g$) to ($1.5L_g$). Besides, it was range about (9.1) % and (13.5) % when reducing the spacing from ($1.5L_g$) to (L_g) under the same value of maximum Froude number. The depth of the sand bed ripples behind the groyne was observed to be about (2.5–3.5) cm.

Based on experimental data obtained, the derived formula for the maximum scours depth ratio of gives a good determination coefficient (0.962) and can be used to evaluate the maximum depth of scour under similar conditions.

9. ACKNOWLEDGMENTS

We thank anonymous reviewers for the valuable suggestions, which helped us improve the quality of our paper. All hydrological data was acquired from the laboratory of Hydraulic in civil Eng. Department, Basrah University.

10. REFERENCES

[1] Abdalla M. G., Study on scour for irrigation canals in Egypt, Case study: The first reach of el-ibrahimeya cana, American Journal of Engineering and Technology Management, Mansoura University, Mansoura, Egypt, Vol.1, No.4, 2017, pp.65-77.

[2] Mostafa M. M., Ahmed H. S. H., Abd-Elraheem G. A., Ali N. A., and Tominaga A.,Experimental study on flow characteristics around single groyne with different permeability in compound channel floodplai, In Proceedings of 2013 IAHR Congress, Tsinghua University Press, Beijin, China, 2013.

[3] Lu J. Y., Hong J. H., Su C. C., Wang c. y., and Lai J. S., Field measurements and simulation of bridge scour depth variations during flood, Journal of Hydraulic Engineering, ASCE, Vol.134, No.6, 2008, pp.810-821.

[4] Khassaf S. I. and Obied N.A., Experimental study: Bridge pier protection against local scour using guide panel, IOP Conference Series: Materials Science and Engineering, Vol. 433, No. 1, 2018.

[5] Melville B., W., and Coleman S., E., Bridge scou, Water Resources Publications, LLC, Colorado, U S A, 2000, pp. 550.

[6] Srivastava S., Pier scouring under live-bed conditio, International Journal of Science Technology & Engineering, Vol.2, No.11, 2016.

[7] Arneson L. A., Zevenbergen L. W., Lagasse P. F., Clopper P. E., Evaluating scour at bridge, Journal of Hydraulic Engineering, United States. Federal Highway Administration, No.18, 2012.

[8] Fathi A., and Zomorodian S. M. A., Effect of Submerged Vanes on Scour Around a Bridge Abutmen, KSCE Journal of Civil Engineering, Korean Society of Civil Engineers, Vol. 22, No.7, 2018, pp.2281-2289.

[9] Hong Y. M., Chang M. L., Lin H. C., Kan Y. C., and Lin C. C., Experimental study on clear water scour around bridge pier, In Applied Mechanics and Materials, Trans Tech Publications Ltd., Vol.121, 2012, pp.162-166.

[10] Ji1a H. J. S., and Karmacharya B., Flood control measures best practices report an approach for community-based flood control measures in the terai river, first edition, German Technical Cooperation, Kathmandu, Nepal, 2000.

[11] Möws R., and Koll K., Roughness effect of submerged groyne fields with varying length, groyne distance, and groyne type, Journal of Water, Vol.11, No. 6, 2019.

[12] Zhang h., and Nakagawa h., scour around spur dyke: journal of advanced and future researches, japan, no.51b, 2008, pp.633-652.